The effect of reverberation on the damping of bubbles

T. G. Leighton,[a] P. R. White, C. L. Morfey, and J. W. L. Clarke
Institute of Sound and Vibration Research, University of Southampton, Highfield, Southampton SO17 1BJ, United Kingdom

G. J. Heald
QinetiQ, Sound Concepts Department, Winfrith Technology Centre, Building A22, Winfrith Newburgh, Dorchester, Dorset DT2 8XJ, United Kingdom

H. A. Dumbrell
QinetiQ, Offshore and Acoustics Department, Newton Road, Bincleaves, Weymouth, Dorset DT4 8UR, United Kingdom

K. R. Holland
Institute of Sound and Vibration Research, University of Southampton, Highfield, Southampton SO17 1BJ, United Kingdom

(Received 27 July 1998; revised 23 January 2002; accepted 26 June 2002)

The measurement of an acoustic emission, or scatter, from a bubble is not difficult. However, an accurate interpretation of that signal in terms of the bubble dynamics may require careful consideration. The study presented here is at first sight relatively simple: comparison of the predicted and measured quality factors of injected bubbles. While the measurement is normally done by monitoring the decay of passive emissions from a bubble, this technique becomes difficult with smaller bubbles. Therefore an active technique is introduced, which removes all the frequency-dependent effects on the measurement (such as transducer response) bar one. That, critically, is the effect of the change in the bubble resonance (frequency and damping) which results from the loading on the bubble due to the reverberant field. The vast majority of theoretical treatments of bubble acoustics assume free field conditions, yet the environmental conditions rarely if ever match these. Therefore measurements of bubble damping are compared both with the established free field theory, and with a new theory relevant to the prevailing reverberant conditions (whether caused by tank surfaces, monochromatic neighboring bubbles, or both). [DOI: 10.1121/1.1501895]

PACS numbers: 43.30.Jx, 43.30.Ft [DLB]

I. INTRODUCTION

It is usually supposed that one of the simplest experiments in bubble acoustics is the estimation of the equilibrium radius of the bubble (R) and its quality factor (Q) from the exponentially decaying sinusoidal pressure trace obtained when an air bubble is injected into water. The use of formulations resembling those of Minnaert[1] or Devin[2] is almost taken for granted in many tests. For example, to the authors' knowledge, all sparging studies on the use of passive acoustic emissions to characterize the bubble population cite Minnaert's equation at the outset[3–8] (with the exception of those which eschew equations[9,10]). Sparging experiments (and indeed almost all such tank tests involving the low kilohertz regime) include reverberation, yet like the vast majority of papers on bubble acoustics the assumption of free-field conditions, implicit in the underlying formulations, is not questioned. This is true throughout the topic, extending to the application of nonlinear equations of motion describing high amplitude bubble oscillation.

For the particular and common task of inferring bubble size from its resonance or natural frequency, the authors[11] previously showed that the presence of a reverberant field could lead to significant errors if free-field formulations, such as that of Minnaert, were used. In the present paper, the rather more difficult problem of calculating the effect of reverberation on bubble damping is attempted. The importance of this work can be judged by considering the following: There are few end-point equations in bubble acoustics that do not incorporate the resonance frequency and damping; and there are few measurements taken in the strictly free-field conditions upon which the common methods of calculating the resonance characteristics are based. Reverberation can arise from the free surface, or from neighboring bubbles, and even from ''anechoically lined'' container walls since these have limitations with respect to absorption and frequency range.

The simplest way of describing bubble damping is through use of a dimensionless damping coefficient,[2,12–15] δ_{tot} (otherwise known as a loss factor). This parameter equals the sum of three dimensionless damping coefficients, corresponding to viscous losses (δ_{vis}), thermal losses (δ_{th}), and the acoustic radiation from the bubble itself (δ_{rad}). For linear systems at resonance, δ_{tot} represents the reciprocal of the quality factor, Q. Despite the fact that the damping coefficient is very widely used, it is not always appreciated that the standard formulations[2,14,15] are valid for monochromatic

[a]Electronic mail: tgl@soton.ac.uk

 0001-4966/2002/112(4)/1366/11/$19.00

bubble pulsations only (which means the steady state linear response to a single-frequency excitation) in the free field. Even the more sophisticated studies[16–21] available, which would for example allow the calculation of damping during the interval prior to steady state, still maintain an assumption of free-field conditions.

Section II describes the general theory. This is followed by an image interpretation. The technique for measuring in isolation the effect of reverberation on bubble damping is then described.

II. METHOD

Section II A gives the general theory for the effect of reverberation on the fluid loading impedance on a small bubble in a test tank of rectangular cross section. Section II B describes the implications of this theory with respect to the effect of reverberation on the bubble resonance frequency and radiation damping. Section II C describes an image technique for calculating the effect which the tank surfaces and any neighboring bubbles have on the resonance of each bubble in a population in monochromatic conditions. Section II D describes a new experimental method for taking measurements in a reverberant tank, which eliminates all the effects of reverberation except for the loading on the bubble wall, making it possible to study this effect in isolation.

A. Theory for the radiation loading on a small bubble in a tank

The impedance presented to a spherically pulsating bubble, radius R, is estimated from the average pressure on a sphere of radius R that surrounds a point monopole having the same volume velocity as the bubble. Consider a liquid-filled rectangular tank that has rigid walls except for the upper surface, which is assumed to be pressure-release. The complex eigenvalues of the tank are denoted by K_N^2. These are the forced-mode eigenvalues, and depend in principle on the forcing frequency. However since this paper is concerned only with modes which exhibit low damping and resonant behavior, the exact frequency dependence of K_N^2 is not critical provided its value can be modeled close to resonance. Let $k_0=\omega/c$ be the acoustic wave number corresponding to acoustic phase speed c and angular frequency ω, and η_N be the loss factor for mode N (defined as the ratio of the imaginary and real parts of K_N^2, at resonance). Then (assuming an implicit time factor of $e^{j\omega t}$)

$$K_N^2=k_N^2+jk_0k_N\eta_N \quad (k_N \text{ real};\ N=1,2,3,\ldots). \tag{1}$$

The analysis that follows allows ck_N to be interpreted as the mode resonance frequency, provided $\eta_N \ll 1$. The first stage of the analysis requires derivation of the acoustic impedance presented to a pulsating spherical surface in this environment [Eq. (6)]. This equation is derived in greater detail by Morse and Ingard[22] [their Eq. (9.4.6)], but an outline derivation is given here to assist understanding of the terms in Eq. (6).

The pressure at point $\boldsymbol{x}$ in the tank, due to a point volume velocity source at point $\boldsymbol{x}_0$, is given[22] by

$$p(\mathbf{x})=\frac{j\omega\rho U}{V}\sum_{N=1}^{\infty}\frac{\psi_N(\mathbf{x})\psi_N(\mathbf{x}_0)}{\Lambda_N(K_N^2-k_0^2)}. \tag{2}$$

Here U is the source volume velocity; the mode shape functions, $\psi_N(\mathbf{x})$, are evaluated at the positions of the receiver $(\mathbf{x})$ and the source $(\mathbf{x}_0)$; and Λ_N is a normalization constant defined by

$$\int \psi_N^2(\mathbf{x})dV=\Lambda_N V, \tag{3}$$

where V is the volume of the tank. The average pressure on a small spherical surface of radius R, centered on the source, can be evaluated explicitly in the low-frequency limit ($k_0R\to 0$) using the expression for $p(\mathbf{x})$ in Eq. (2). The result is[22]

$$\langle p(R)\rangle \approx \frac{j\omega\rho}{4\pi R}U \quad \left(k_0R\to 0;\quad R\ll\frac{k_0^2V}{4\pi}\right); \tag{4}$$

provided that the mode with $k_N=0$ (for a hard-walled cavity) is not included.[23]

Equation (4) is the free-field result, as expected. It follows that if $k_0R\ll 1$ (but has a finite value), and if the tank is sufficiently large for Eq. (4) to be valid (i.e., $k_0^2V\gg 4\pi R$), then an improved approximation is

$$\begin{aligned}\langle p(R)\rangle &\approx \frac{j\omega\rho}{4\pi R}U+\langle p(R)\rangle|_{k_0R}-\langle p(R)\rangle|_0\\ &=j\omega\rho U\left(\frac{1}{4\pi R}+\frac{1}{V}\sum_{N=1}^{\infty}\frac{1}{\Lambda_N}\psi_N^2(\mathbf{x}_0)\right.\\ &\quad\left.\times\left(\frac{1}{K_N^2-k_0^2}-\frac{1}{K_N^2}\right)\right),\end{aligned} \tag{5}$$

where vector $\mathbf{x}_0$ is the position of the center of the sphere, and the difference between ψ_N at the center and ψ_N on the surface has been neglected.[24] The fluid loading impedance on a small bubble in a tank can now be estimated by dividing both sides of Eq. (5) by U and simplifying:

$$Z_s=\frac{\langle p(R)\rangle}{U}\approx j\omega\rho\left(\frac{1}{4\pi R}+\frac{k_0^2}{V}\sum_{N=1}^{\infty}\frac{\psi_N^2(\mathbf{x}_0)}{\Lambda_N K_N^2(K_N^2-k_0^2)}\right)$$
$$(k_0R\ll 1). \tag{6}$$

This expression is the Morse and Ingard result [Eq. (9.4.6)] for the acoustic impedance presented to a pulsating spherical surface of radius R, which represents a single bubble in the tank.

The first term in the brackets on the right-hand side of Eq. (6) is purely reactive; it dominates in the limit $k_0R\to 0$. However, it simply represents the free-field inertial fluid loading on the bubble. What is more interesting is the deviation from the free-field impedance, as given by the modal summation terms. In particular, the bubble radiation damping comes entirely from the modal summation terms (note that no local viscous or thermal damping has been included at this stage). At low frequencies, the resistance $Z_s^R=\mathrm{Re}(Z_s)$ consists of a sequence of resonant modal peaks. At suffi-

ciently high frequencies the overlap of many modal peaks will produce a smooth curve, corresponding to

$$Z_s^R \approx \frac{\rho c k_0^2}{4\pi}, \tag{7}$$

which is equivalent to the free-field radiation resistance. This last result is derived in the analysis that follows [see Eq. (30)].

The modal loss factors and resonance frequencies can be found experimentally from transmission measurements in the tank. Note from Eq. (2) that, in the neighborhood of a resonance, the pressure at $\mathbf{x}$ due to a point source at $\mathbf{x}_0$ will vary as

$$p(\mathbf{x}) \propto \frac{1}{K_N^2 - k_0^2} = \frac{1}{(k_N^2 - k_0^2) + j\,\eta_N k_N k_0} = \frac{1}{D}, \tag{8}$$

where the denominator D describes the resonance.

At the modal peak, $k_N = k_0$. Therefore at the half-power points on the resonance curve,

$$|k_N^2 - k_0^2| = \eta_N k_N k_0, \tag{9}$$

i.e.,

$$|k_N - k_0| \approx \tfrac{1}{2}\eta_N k_N \quad (\eta_N \ll 1). \tag{10}$$

It follows that the quality factor for the Nth mode of the tank is equal to η_N^{-1}. Once this is known, the real and imaginary parts of Z_s can be found explicitly from Eq. (6). Provided the loss factors η_N are small, and omitting terms in η_N^2 (except where they occur in $|D|^2$, in the following) the resistance can be approximated by

$$Z_s^R \approx \frac{\rho c}{k_0 V} \sum_{N=1}^{\infty} S_N, \tag{11}$$

where

$$S_N = \frac{\psi_N^2(\mathbf{x}_0)}{\Lambda_N} \frac{(2-\nu_N^2)\,\eta_N \nu_N^5}{|D|^2}. \tag{12}$$

Here $|D|^2 = (1-\nu_N^2)^2 + (\eta_N \nu_N)^2$ and $\nu_N = k_0/k_N$ is the ratio of the driving frequency to the resonance frequency of mode N. In a similar way the reactance can be approximated by

$$Z_s^I = \mathrm{Im}(Z_s) \approx \frac{\omega \rho}{4\pi R} + \frac{\rho c}{k_0 V} \sum_{N=1}^{\infty} T_N, \tag{13}$$

where

$$T_N = \frac{\psi_N^2(\mathbf{x}_0)}{\Lambda_N} \frac{(1-\nu_N^2)\,\nu_N^4}{|D|^2}. \tag{14}$$

Note that the modal summation terms S_N in the resistance, Eq. (12), exhibit resonance, while the T_N terms in the reactance vanish at resonance [i.e., when $\nu_N = 1$; Eq. (14)].

For modes of very high order, i.e., $k_N \to \infty$ or $\nu_N \to 0$, the summation terms S_N of Eq. (11) behave like

$$S_N \sim \nu_N^5 \tag{15}$$

and the summation terms T_N of Eq. (13) behave like

$$T_N \sim \nu_N^4. \tag{16}$$

There should therefore be no problem over convergence. We can check this by using the asymptotic relations

$$N \sim k_N^3 - \nu_N^{-3}, \quad \frac{dN}{d\nu_N} = n(\nu_N) \sim \nu_N^{-4}. \tag{17}$$

The product of the modal density $n(\nu_N)$ with S_N or T_N remains finite, in the limit $\nu_N \to 0$.

Note that the sums in Eqs. (11) and (13) extend from $N=1$ to $N=\infty$ over integer N. They may be estimated beyond some lower limit N_0 by replacing the sum over N with an integral over ν that involves the modal density $n(\nu)$:

$$\sum_{N=N_0}^{\infty} S_N \simeq \int_{\nu_0}^{0} S(\nu) n(\nu)\, d\nu, \tag{18}$$

and similarly for $\Sigma_{N=N_0}^{\infty} T_N$. The lower limit ν_0 is given by

$$\nu_0 = k_0 L_0, \tag{19}$$

where L_0 is the length that characterizes the tank dimensions. Thus ν_0 is a dimensionless frequency above which the modes of the tank are sufficiently close-spaced to be regarded as a continuum for the purposes of Eqs. (11) and (13). The upper limits of the integrals are zero, corresponding to $k_N \to \infty$.

Note that the modal density $n(\nu)$ follows from the asymptotic mode count $N(k)$:

$$N(k) \simeq \frac{k^3 V}{6\pi^2}, \tag{20}$$

where V is the tank volume. Thus

$$N(k_N) = \frac{k_N^3 V}{6\pi^2} = \left(\frac{k_0}{\nu_N}\right)^3 \frac{V}{6\pi^2}, \tag{21}$$

and

$$\frac{dN}{d\nu} = -\frac{k_0^3 V}{2\pi^2} \nu^{-4} = n(\nu), \tag{22}$$

by definition. In Eq. (22) ν is regarded as a continuous variable. Replacement of the summation step ($\Delta N = 1$) in Eqs. (11) and (13) by an integration increment, $dN = n(\nu)\,d\nu$, leads to Eq. (18).

The final expression for Z_s, based on summation of Eqs. (11) and (13) up to mode N_0, followed by the integral approximation of Eq. (14) for $N > N_0$, is as follows. The real component of Z_s is

$$Z_s^R = \frac{\rho c}{k_0 V}\left(\sum_{N=1}^{N_0} S_N + \frac{k_0^3 V}{2\pi^2} \int_0^{\nu_0} \frac{(2-\nu^2)\,\eta\nu}{(1-\nu^2)^2 + \eta^2\nu^2}\, d\nu \right), \tag{23}$$

and the imaginary component is

$$Z_s^I = \frac{\omega\rho}{4\pi R} + \frac{\rho c}{k_0 V}\left(\sum_{N=1}^{N_0} T_N + \frac{k_0^3 V}{2\pi^2}\int_0^{\nu_0} \frac{(1-\nu^2)}{(1-\nu^2)^2+\eta^2\nu^2}\, d\nu \right). \quad (24)$$

To obtain Eqs. (23) and (24), Eq. (22) for $n(\nu)$ has been substituted into Eq. (18). The expressions for $S(\nu)$ and $T(\nu)$, Eqs. (12) and (14), have been approximated by replacing $\psi_N^2(\mathbf{x}_0)/\Lambda_N$ with its average value of unity.

Equations (23) and (24) are the main results of the theoretical analysis of this section. Two limiting cases can usefully be distinguished, corresponding to low and high frequencies. In the low frequency limit, defined by

$$k_0 L_0 = \nu_0 \ll 1, \quad (25)$$

the contribution of the integral terms is small compared with that of the summation terms. Note that the integrals in this case do not pass through any resonances.

In the high frequency limit, defined by

$$k_0 L_0 = \nu_0 \gg 1, \quad (26)$$

the contribution of the integral terms is dominant. Provided the overlap of individual-mode responses is sufficient to justify the continuous-distribution model, particularly in the region close to resonance ($\nu \approx 1$) where the integrands are largest, we can estimate the resistance and reactance as follows:

$$Z_s^R \simeq \frac{\rho c k_0^2}{2\pi^2} I_{\text{res}} \frac{\pi}{2}\, \eta_{\text{res}}, \quad (27)$$

$$Z_s^I \simeq \frac{\omega\rho}{4\pi R}. \quad (28)$$

Note that the integral contribution in Eq. (24) tends to cancel either side of $\nu \approx 1$, which is why Eq. (28) gives just the free field value. In Eq. (27), I_{res} represents the value of the integrand in Eq. (23) at the resonant peak, i.e.,

$$I_{\text{res}} = \frac{1}{\eta_{\text{res}}} \quad (\nu = 1). \quad (29)$$

Thus

$$Z_s^R(\text{high frequency}) \simeq \frac{\rho c k_0^2}{4\pi}, \quad (30)$$

which is the free field value (as expected).

B. Practical implications

The practical implications of the radiation loading result of Eqs. (11) and (13) are interesting, in terms of estimating the bubble radius and damping from the measured acoustic emissions of a single bubble. We define Z_b as the acoustic impedance of the bubble,[25] that is, the ratio of the pressure change Δp to the inwards volume velocity at the bubble wall. If Z_a is the external acoustic impedance due to fluid loading on the bubble, then resonance occurs when

$$Z_a + Z_b = 0. \quad (31)$$

Equation (31) can be used to determine the relationship between the pulsation resonance frequency and the equilibrium bubble radius. For example, since the apparent bulk modulus of the gas within the bubble (of volume V_b) when subject to a pressure change Δp is $B = -V_b \Delta p/\Delta V_b$, then assuming single-frequency simple harmonic motion at circular frequency ω, the acoustic impedance of the bubble at low frequencies ($k_0 R \ll 1$) is

$$Z_b \approx \frac{\Delta p}{-U} = \frac{\Delta p}{-j\omega \Delta V_b} = \frac{B}{j\omega V_b}. \quad (32)$$

If the gas within the spherical bubble is assumed to behave polytropically (i.e., $pV^\kappa = \text{constant}$), then $B = \kappa p_0$, where p_0 is the ambient static pressure on the bubble and κ is the polytropic index. The bubble at resonance ($\omega = \omega_0$) is described by Eq. (31) (where in the reverberant conditions of the tank, Z_a is described by Z_s from Sec. II A). If damping is small and hence the resistive terms are neglected, then Z_a and Z_b are almost entirely reactive, ω_0 is real, and Eq. (13) gives

$$\frac{j\kappa p_0}{\omega_0 V_b} \approx j\omega_0 \rho \left(\frac{1}{4\pi R} + \frac{1}{k_0^2 V} \sum_{N=1}^{\infty} T_N \right) \quad (k_0 R \ll 1), \quad (33)$$

where T_N is defined in Eq. (14). The summation term in Eq. (33) represents a reverberant-field correction to the free-field radiation reactance. Neglecting the correction leads to the free-field expression for the resonance frequency of the bubble:[1]

$$\omega_0 \simeq \sqrt{\frac{4\pi R \kappa p_0}{\rho V_b}} = \frac{1}{R}\sqrt{\frac{3\kappa p_0}{\rho}} = \omega_{0f}. \quad (34)$$

An improved approximation is found by evaluating the reverberant correction term at the Minnaert frequency ω_{0f}. The corrected resonance frequency for bubble pulsation in a tank follows from Eq. (34), with the substitution

$$\frac{1}{R} \to \frac{1}{R} + \frac{4\pi c^2}{\omega_{0f}^2 V} \sum_{N=1}^{\infty} T_{Nf} = \frac{1}{R} + \frac{4\pi\rho c^2}{3\kappa p_0 V} R^2 \sum_{N=1}^{\infty} T_{Nf}. \quad (35)$$

Here T_{Nf} denotes T_N of Eq. (14) evaluated at $\omega_0 = \omega_{0f}$. The presence of the summation in Eq. (35) can be seen as a correction which modifies the "free-field" resonance frequency for bubble pulsation. A similar correction factor was used by Leighton *et al.*[11] to modify free-field theory, and thus to estimate the bubble size from the resonance frequency measured in reverberant conditions in a pipe.

However there is a critical difference when calculating how the presence of reverberation changes the bubble damping. As can be seen from Eq. (11) there is no equivalent free-field term: the radiation damping result is entirely made up of the summation terms, and hence the modal structure of the field has to be very well characterized to evaluate this. This can be attempted by measuring the character of the sound field (removing, of course, transducer response, etc., see Sec. II C) and identifying the component modes through

use of Eq. (5). The data can then be converted into effective measurements of the radiation resistance. An alternative but equivalent approach to estimating the reverberation effect is described in Sec. II C. Here an image model is used to calculate the effect of tank surfaces on the radiation impedance of a single oscillating bubble. The technique can also be used to characterize the resonance of each bubble in a *population* driven to steady state by some external source: the effect on each bubble of both the tank's surfaces and of the neighboring bubbles can be incorporated.

C. Method of images

The effect of neighboring reflective boundaries on the radiation impedance of a bubble can be modeled using the method of images. For the specific case of the tank of rectangular cross-section discussed in Sec. II A, the location of the images is calculated from the position of the bubble relative to each wall, the result being an infinite number of images arranged in a grid-like pattern. If the complex pressure reflection coefficient of the various tank walls were of unit magnitude for the frequencies emitted by the bubble, then a continuously emitting bubble would of course generate reverberant acoustic intensities at the bubble surface which would grow with time. This produces a coherent radiation version of Olbers' paradox,[26] by which Halley, Cheseaux, and Olbers realized that, if the number density of stars were constant and the absorption of light in interstellar space were negligible, then unless the universe were finite, the night sky would generate at the observer an intensity equal to the average surface intensity of the stars.

The pressure field radiated by the bubble p consists of a direct field p_d and a reverberant one p_ν:

$$p = p_d + p_\nu, \tag{36}$$

where in the condition $k_0 R \ll 1$ the reverberant field is virtually constant over the bubble surface and very similar to that produced at the bubble center location by a point source having the same volume velocity as the bubble. The total acoustic impedance presented to the bubble, Z_a, is

$$Z_a = \frac{p}{U} = \frac{p_d}{U} + \frac{p_\nu}{U}, \tag{37}$$

where p_d is the direct field on the bubble surface:

$$p_d = \frac{j\rho\omega}{4\pi R} + \frac{\rho\omega^2}{4\pi c} \quad (k_0 R \ll 1) \tag{38}$$

(suppressing the harmonic time dependence throughout). Consider two bubbles emitting monochromatic monopole ($kR \ll 1$) radiation, the first having volume velocity U and the second having source strength FU. The pressure at bubble 1 as a result of the radiation from bubble 2 is

$$p_{12} = j\omega\rho F U\left(\frac{e^{-jkr}}{4\pi r}\right), \tag{39}$$

where the bubble separation r introduces both a phase factor and an attenuation. The impedance of Eq. (38) resulting from a population of monochromatic bubbles is therefore

$$\begin{aligned} Z_a &= \frac{j\rho\omega}{4\pi R} + \frac{\rho\omega^2}{4\pi c} + \frac{j\rho\omega}{4\pi}\sum_{m=2}^{m_{\max}} \frac{F_m}{r_m} e^{-jkr_m} \\ &= \frac{j\rho\omega}{4\pi R} + \frac{\rho\omega^2}{4\pi c} + \frac{\rho\omega}{4\pi}\sum_{m=2}^{m_{\max}} \frac{|F_m|}{r_m}(\sin(kr_m - \vartheta_m) \\ &\quad + j\,\cos(kr_m - \vartheta_m)), \end{aligned} \tag{40}$$

where the subscript $m = 2,3,\ldots,m_{\max}$ indicates all bubbles other than bubble 1. These entities may be real bubbles driven linearly at steady state by an external monochromatic source. Equation (40) might also describe the impedance of a single bubble in a tank (where the bubbles $m = 2,3,\ldots,\infty$ are images); or indeed be used to calculate the resonance characteristics of each bubble in a monochromatic population within a tank (in which case the population comprises both real and image bubbles). To compare with the calculation of Sec. II A and II B, a single bubble in a rectangular tank would have images characterized by a range term r_m (equal to twice the shortest distance between the real bubble and the wall); and a complex amplitude term $F_m = |F_m| e^{-j(k_m r_m - \vartheta_m)}$ which would depend on the complex reflection coefficient of the boundary in question. Then if the small-damping polytropic conditions of Sec. II B apply, the resonance condition occurs when

$$\begin{aligned} \frac{j\kappa p_0}{\omega_0 V} &\approx \frac{j\rho\omega}{4\pi R} + \frac{\rho\omega^2}{4\pi c} + \frac{\rho\omega}{4\pi}\sum_{m=2}^{\infty} \frac{|F_m|}{r_m}(\sin(kr_m - \vartheta_m) \\ &\quad + j\,\cos(kr_m - \vartheta_m)). \end{aligned} \tag{41}$$

Equating the imaginary parts gives the resonance frequency

$$\omega_0 \approx \frac{(1/R)\sqrt{3\kappa p_0/\rho}}{\sqrt{1 + \Sigma_{m=2}^{\infty}(R/r_m)|F_m|\cos(kr_m - \vartheta_m)}}, \tag{42}$$

which reduces to the Minnaert equation [Eq. (34)] when, in the free field, the summation term is zero.

The effect of neighboring bubbles and boundaries on radiation damping can also be calculated by this method. Assume that the radiation damping in free space is to be characterized by the dimensionless damping coefficient, $\delta_{\text{rad,free}}$, which is proportional to the real part of the total acoustic impedance presented to the bubble in free space, $\rho\omega^2/4\pi c = \rho\omega k/4\pi$. The ratio of the damping in reverberant conditions, $\delta_{\text{rad,reverb}}$, to that in free space, equals the ratio of the real parts of the respective total acoustic impedances presented to the bubble. Taking again the case of Sec. II A (a single bubble emitting into a rectangular tank) the ratio of the real component of Eq. (41) to the free-space value is

$$\frac{\delta_{\text{rad,reverb}}}{\delta_{\text{rad,free}}} = 1 + \sum_{m=2}^{\infty} \frac{|F_m|\sin(kr_m - \vartheta_m)}{kr_m}. \tag{43}$$

For solution of the tank case described in Sec. II A and Eqs. (42) and (43), the spatial distribution of the images is calculated geometrically, and the frequency-dependent complex reflection coefficient associated with each image is simply calculated from the number of reflections from the tank boundaries. The predicted quality factor for a bubble in reverberant conditions is then

$$Q = 1/\delta_{\text{tot}} = 1/(\delta_{\text{rad,reverb}} + \delta_{\text{th}} + \delta_{\text{vis}}), \tag{44}$$

where δ_{th} and δ_{vis} are found from the usual monochromatic formulations,[2] and where $\delta_{\text{rad,reverb}}$ is calculated by substituting into Eq. (43) the monochromatic value of $\delta_{\text{rad,free}}$, again calculated from literature.[2]

With reference to the comments at the start of this section, it should be noted that Eqs. (42) and (43) assume that the emission from the images is steady. If for example the source bubble emits an exponentially decaying sinusoid typical of injection, then the nonsteady nature of the returns introduces an error of order δ_{tot}^2.

D. Experimental measurements

The method used in this paper for measuring the bubble resonance and damping relies upon estimation of the impulse response of bubbles injected one at a time into a tank measuring 0.6 m×0.2 m×0.23 m deep internally, and having glass walls of 6 mm thickness. For the ''passive'' technique, this consisted of simply measuring the hydrophone signal detected following injection of the bubble through a needle. For the ''active'' technique, the hydrophone signal of interest is not that emitted by the bubble on injection. Rather, it is the signal scattered by the bubble some time later, when it is driven by band filtered white noise (1–25 kHz, generated using a Bruel and Kjaer Type 2032 dual channel signal analyzer). The bubbles examined in this paper have natural frequencies in the range 4–11 kHz. The bubble rises after injection, and is driven into oscillation by the pseudorandom driving field. Its buoyant passage through a 1 MHz beam triggers the data acquisition from the hydrophone. It is important to know the location of the bubble and hydrophone for comparison with theory. The active technique is particularly useful in measuring the resonance characteristics of the smaller bubbles, whose natural emissions after injection are of insufficient amplitude above the noise to obtain sufficient cycles for a precise measurement of their decay. The following describes how the scattered signal is estimated when the active technique is used.

The received signal at the measurement hydrophone, $y(t)$, in the active configuration, can be considered as the superposition of two components, i.e.,

$$y(t) = y_d(t) + y_s(t), \tag{45}$$

where $y_d(t)$ is the signal due to the direct field (i.e., the signal that is observed in the absence of a bubble), and $y_s(t)$ is the signal arising from the acoustic field generated by scattering from the bubble. In practice the magnitude of the direct field component is sufficient to corrupt measurements of quantities, such as quality factors, based on the raw data $y(t)$. If no bubble is present, then evidently the measured signal is solely due to the direct field component, $y_d(t)$.

Figure 1(a) illustrates a typical example of the spectrum of a signal received at a hydrophone when an active configuration is employed with a bubble being present. The spectrum of the electronic signal used to drive the projector (band limited Gaussian noise) is also shown. The resulting hydrophone signal contains contributions from the direct field and the scattered signal. The ''N''-shaped feature at approximately 3 kHz is a result of bubble scattering.[27] The problems of exploiting this data are evident. The comparatively low level of the scattered signal relative to the direct field render the feature difficult to discern even in this relatively small frequency range (its peak is of a similar magnitude to the nonbubble feature at around 6 kHz); and estimation of the bubble quality factor from such a feature is prone to error (see the following). Our methodology aims to reduce the direct field contribution and allow accurate measurements to be made.

To estimate the scattered field we first make measurements in the *absence* of a bubble. A known band limited white noise signal, $x(t)$, is used as an input to the projector and the resulting hydrophone signal is measured. Using standard linear systems theory[28] we can construct an estimate of the system impulse response, $h_d(t)$, from these two measurements. Assuming that the modeling is successful then

$$y_d(t) = h(t) * x(t), \tag{46}$$

where an asterisk is used to denote linear convolution. The accuracy of the model can be assessed as a function of frequency by computing and examining the coherence function.[28]

A bubble is then introduced to the system. Once again a band limited white noise signal, $x(t)$, is used to drive the projector. From the driving signal an estimate of the direct field component of the hydrophone signal is constructed by convolving it with the estimated impulse response, $h(t)$, leading to an estimate of the scattered signal:

$$\hat{y}_s(t) = y(t) - h(t) * x(t). \tag{47}$$

Here $\hat{y}_s(t)$ is an estimate of the contribution of the bubble to the acoustic field. The results of applying this procedure to the data in Fig. 1(a) are shown in Fig. 1(b). The spectrum of the signal after the effect of the direct field has been subtracted shows a distinct peak close to 3 kHz, for which the ratio of center frequency to the bandwidth gives the bubble quality factor. Figure 1(b) illustrates the error that would have been introduced if one had erroneously assumed that Q could be obtained from the equivalent parameters associated with the 3 kHz peak in Fig. 1(a).

This model takes account of any shaping of the excitation spectrum that may occur as a result of a modal field within the tank. This having been removed, what remains is the effect of reverberant loading on the bubble resonance and damping.

III. RESULTS

Figure 2 shows the quality factor of the bubble as a function of its natural (for the ''passive'' measurements: ■,●) or resonance (for the ''active'' measurements: □,○,×) frequency. Results from tap, distilled, and newly acquired seawater are shown. The solid curve indicates the quality factor predicted by Devin's theory, which relates to free field conditions. The dashed line indicates the result predicted by Eq. (43), with the dotted lines on either side indicating the maximum and minimum values found by recalculating the prediction repeatedly, allowing the bubble position and the wall reflection coefficient to vary within the limits of uncer-

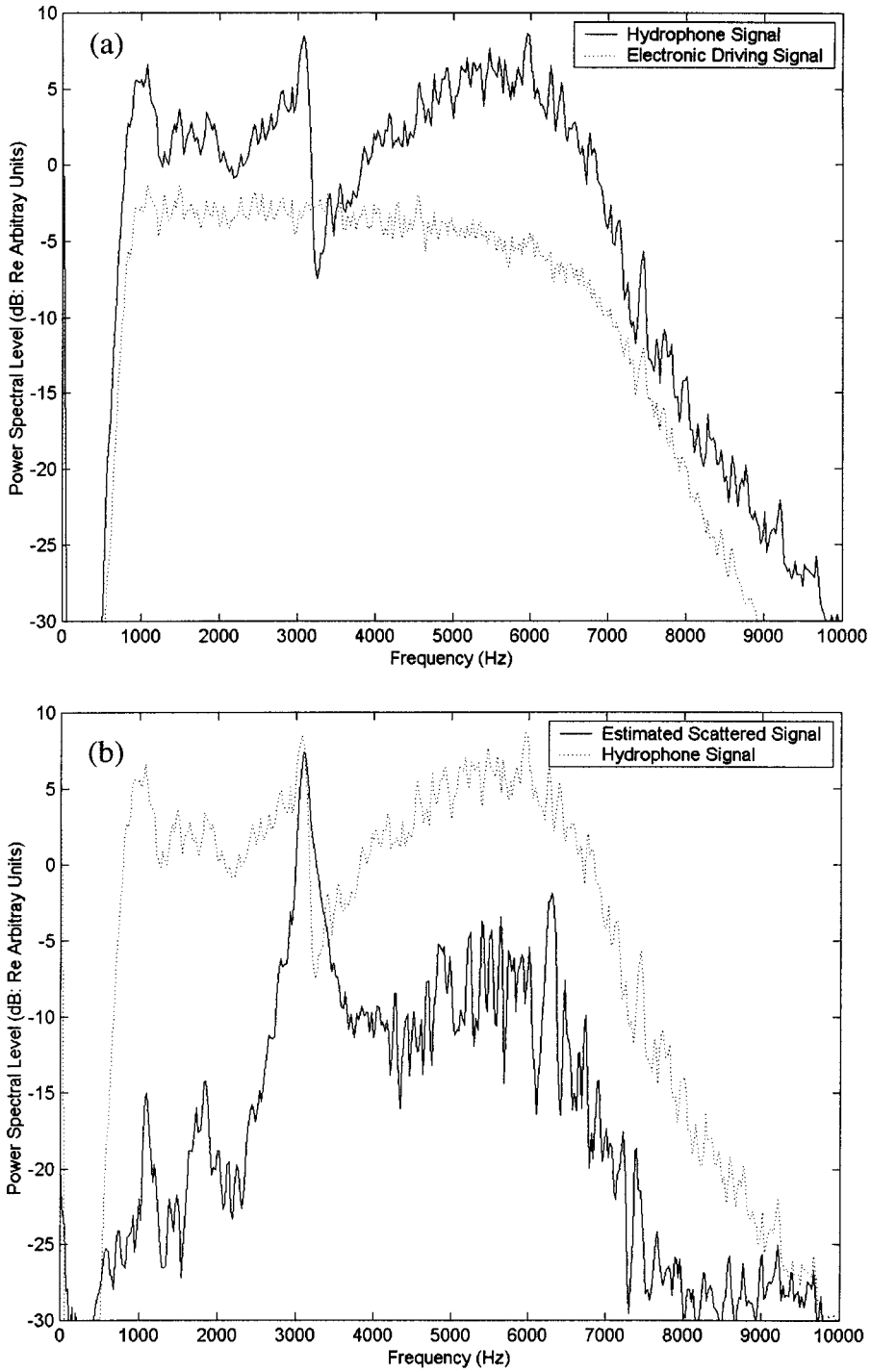

FIG. 1. (a) Spectra of driving signal and hydrophone signal. The driving signal in this example case consists of Gaussian noise, band limited to a frequency range of approximately 1–7 kHz (though 1–25 kHz was required for the data of Fig. 2). (b) Spectra of the hydrophone signal before and after the effect of the direct field has been removed.

tainty of each (the latter having a much smaller contribution that the former, the prediction being fairly robust within the allowed variation of reflection coefficient). For clarity, error bars are not shown (± 75 Hz; ± 1 in Q for $f<6$ kHz; ± 2 in Q for $6<f<9$ kHz; ± 4 in Q for $f>9$ kHz). The lack of passive data above 6 kHz reflects the signal-to-noise problem, described in Sec. II C, which makes the technique difficult for the smaller bubbles. The active technique is not limited in this way.

The discrepancy between observation and the prediction of Devin is less than the error associated with the observation for 26 of the 96 data points. There being negligible uncertainty on this scale in the uncertainty associated with the Devin curve, the conclusion is that Devin's theory is inappropriate for the reverberant conditions found in this typical test tank, in the frequency range most often studied in bubble acoustics. In contrast 76 of the 96 bubbles lie within one error of the theory presented in this paper. This comparison needs interpreting with some caution, as discussed in the following.

IV. DISCUSSION

Although the disagreement between measurement and Devin's theory indicates the need for a theory applicable to reverberant conditions, and while the authors have faith in

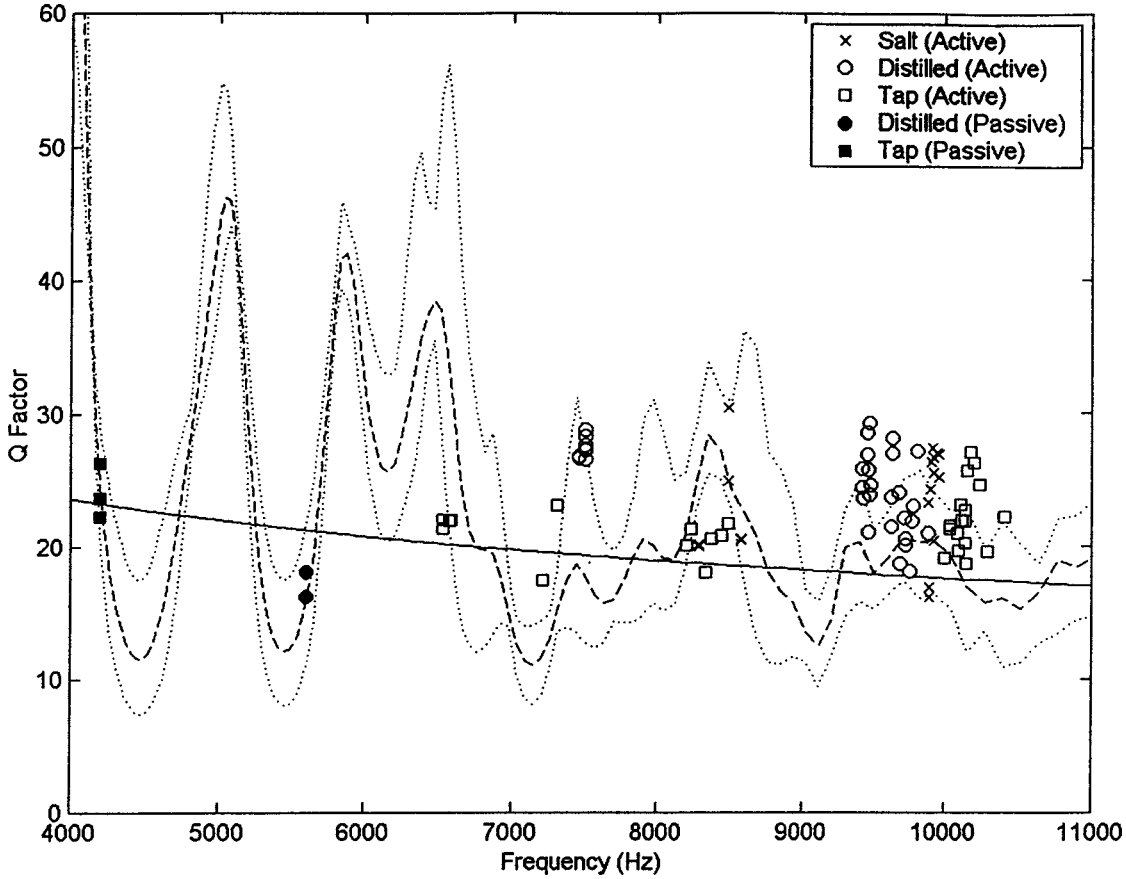

FIG. 2. Graph of the quality factor of the bubble as a function of its natural (for the "passive" measurements, ■, ●) or resonance (for the "active" measurements, □ ○ ×) frequency. Results from tap (■, □), distilled (●, ○) and newly-acquired seawater (×) are shown. For clarity, error bars are not shown (±75 Hz; ±1 in Q for $f<6$ kHz; ±2 in Q for $6<f<9$ kHz; ±4 in Q for $f>9$ kHz). The curves indicate predictions of the theory of Devin (—) and of this paper (---), either side of which is a dotted line indicating the limits of uncertainty in the latter.

the theories of Sec. II, implementation of that theory to calculate the modification to bubble resonance imparted by reverberant loading is not easy. Whereas calculation of the effect on resonance frequency[11] is possible by using Eq. (37), the effect on the damping is very sensitive to details of the reverberation. The resulting uncertainty allows a range of predicted values for Q at each frequency in Fig. 2, while the standard free-field theory predicts a single value. The sensitivity of the prediction to the reverberation parameters is of course greatest at the peaks and troughs in the plots, and hence the extreme predictions of $Q>40$ should be interpreted with caution. For the most part the reverberant theory suggests for this tank there will be deviations from free-field predictions of usually up to $Q\sim 60\%$, and these are observed. In addition the predicted sign of the deviation (which can be positive or negative depending on the frequency) is borne out in the data.

While the magnitude of the discrepancy is difficult to calculate precisely, the form for the quality factor of bubbles in this reverberant environment that is predicted by the method of images technique described in Sec. II C, agrees with the trends expected from the general theory of Sec. II A. Equation (7) predicts that at sufficiently high frequencies, the damping will tend to a smooth function following the "free-field" solution. This is a result of modal overlap. The prediction in Fig. 2 bears this out, although in the range considered the influence of distinct modes is evident. At the lower frequencies the calculation becomes difficult because of convergence problems [note that $|D|^2=(1-\nu_N^2)^2+(\eta_N\nu_N)^2$ in Eqs. (11) and (12) becomes very large when $k_0\rightarrow k_N$, then $\nu_N\rightarrow 1$]. Paradoxically this means that the effect of reverberation can be easier to calculate in small tanks than in larger ones. This is because the bubbles most often considered in test tanks have natural frequencies of the low kilohertz order (see the following). Therefore unless the tank is sufficiently vast and sufficiently damped that this range is higher than the Schroeder frequency, then to ignore reverberation the bubble natural frequency must be significantly less than that of the first tank mode[11] (depending on the losses, which are generally lowest for these low frequencies). In tanks of several meters on a side this in practice would likely occur only for bubbles resonant at O (10 Hz). Such bubbles would generally be much larger than those typically studied in a test tank. It is well-known that if the intention is to inject single bubbles into a tank for controlled tests, there is a range of bubble size outside of which this process becomes difficult. Bubbles of centimeter-size break up, and bubbles of less than around 200 μm tend to coalesce into larger bubbles at the nozzle.[29] Even exotic methods (e.g., manipulation of the surface tension or pressure head, vibration of the needle, etc.) can only expand this range to a

limited degree. Of course smaller bubbles can be produced by sparging, wave breaking,[30] etc., but these bubbles almost always comprise a subset of a population which includes larger bubbles giving significant natural emissions at roughly 1–10 kHz.

As this paper has shown, this may well be a problematic range: the frequencies may be insufficiently high to generate, via model overlap, the effectively ''free-field'' solution of Eq. (7); yet they may be so low that anechoic linings are insufficient to remove reverberation. For example, even with the free surface replaced by lining, the ''anechoically'' lined tank of Bjørnø and Kjeldgaard had a pressure amplitude reflection coefficient of ~0.3 at 10 kHz, the lowest frequency they measured. The actual performance of linings at the frequencies of interest is not always reported in bubble tests.

As an illustration of the problem, a preliminary attempt was made to use the results of Fig. 2 to confirm or counter the suggestion[31,32] that bubble damping may depend on salinity. That suggestion followed from a study of the injection of single bubbles into a tank having ''acoustically transparent'' walls. This smaller tank was suspended in a larger 2.5 $\times 3.6 \times 3.6$ m^3 water tank, where ''the bottom and walls of the [larger] tank were lined with 82-cm high redwood wedges with 30 cm$\times$30 cm bases; these wedges have a large acoustic absorption.''[33] Being cognizant that such statements depend on the frequency of interest, an investigation[33] was made to determine which modes could be excited in the largest tank at frequencies of less than 1 kHz, and identified ones at around 540 and 950 Hz.

It is well known that dissolved salt can affect *populations* of bubbles, those formed in salt water tend to be more numerous, particularly regarding the smallest bubbles, and less prone to coalesce than bubbles in fresh water.[34–39] When comparing wave breaking in fresh water with that in salt, it is one thing to attribute acoustic differences to changes in populations of bubbles which, as individuals, have unchanged acoustic properties. That is to say that, even though the collective effect may be affected by differences between the fresh and salt water bubble populations, the single-bubble acoustics is the same (although modifications may be necessary to surface tension and thermal damping terms, etc., as a result of the ''dirty'' nature of sea water[40]). It is quite another to suggest that the single-bubble dynamics might be different, which is one possible interpretation of the findings of the study[31] mentioned previously. In that, measurements were made of the logarithmic decrement of relatively large single bubbles (1.1–2.4 mm radius) injected into water having a salinity range of $0^{\circ}/_{\circ\circ}$–$35^{\circ}/_{\circ\circ}$ (obtained using commercial salt[41]). Both the sound pressure level and the quality factor were observed to change with salinity, but no mechanism for such a single-bubble effect has been proposed. If such a single-bubble effect was robust (and not, as speculated in the following, a by-product of the reverberation), it would have major implications throughout ocean bubble acoustics, for example in measurements of the bubble population[42–46] and the response of bubbles to short acoustic pulses.[47–50]

Prior to the current paper, no account has been taken in test tanks of the effect of the reverberant field on the bubble damping. That two distinct modes at 540 and 950 Hz could be identified in the tank used in the earlier study[33] suggests that the data were taken in the frequency range (roughly 1–3 kHz) at which the effect of reverberation is most problematic, as discussed previously. Taking reverberation into account, the results of Fig. 2 are unable to confirm or deny the earlier proposition that salinity affects the damping of single bubbles: the seawater data ($\times$) show a similar measure of agreement with the prediction of reverberant theory that is exhibited by tap and distilled water. Hence the disagreement which is seen in this paper between the seawater data and the prediction of Devin can be attributed to reverberation. That is not to prove that reverberation was responsible for the earlier finding.[31,32] However the potential for reverberation to complicate the observation is clear. As an example, even small changes in frequency/sound speed can tune in or out of the effect of a given mode, leading to significant changes in Q (Fig. 2). While varying the salinity will change the sound speed in a predictable manner[51] in single-bubble tests, when *populations* are entrained there is a second, and often greater effect. If changes in salinity affect the population of bubbles entrained, for example by a breaking wave, then varying the salinity will indirectly affect both the amount of reverberation and (through the effect of the bubble population on the sound speed) change the modal frequencies of the tank. Figure 2 suggests that mode frequency changes of O (1%) can cause changes in Q of O (10%). Therefore it is strongly recommended that reverberation be considered in tank tests, and other reverberant environments.[52]

The importance of reverberation on bubble resonances should not be underestimated, and its effect cannot be easily dismissed. It is not confined only to frequencies of tank modes: apart from the frequency region well below the first mode,[11] or well above the Schroeder frequency, the effect is potentially very problematic for three reasons.

(1) Calculation of its influence on radiation damping in particular (and, to a lesser extent, on the relationship between the bubble radius and natural frequency) requires detailed knowledge of the reverberation.
(2) Small changes in damping can have major effects close to bubble resonance, and discrepancies from the free field predictions of up to ~60% are here observed.
(3) True free-field conditions are rarely found in bubble acoustics, with even the ''open'' ocean containing a free-surface, and scatterers which include other bubbles; and ''anechoic'' fittings can give significant reflections at the resonant frequencies of the larger bubbles.

Finally it should be recalled that the ubiquitous assumption of free-field conditions extends beyond bubble entrainment emissions and linear scattering, to the nonlinear models of bubble motion (such as the Rayleigh–Plesset, Herring–Keller, and Gilmore-Akulichev formulations). Certain scenarios exploit modal fields, such as in measurement of the bubble size distribution.[53–55] Of particular note is the common practice of levitating bubbles in a modal sound field for measurements of, for example, sonoluminescence,[56] rectified diffusion,[57] or (with the comment of this paper particularly in mind) resonance and damping.[58,59] In such circumstances the

effect and validity of the free-field assumption must be assessed.

ACKNOWLEDGMENTS

The authors would like to acknowledge the support of QINETIQ, Bincleaves, UK. T.G.L. is grateful to the Royal Society Leverhulme Trust, and the EPSRC (GR/M38094) for support.

[1] M. Minnaert, "On musical air-bubbles and sounds of running water," Philos. Mag. **16**, 235–248 (1933).
[2] C. Devin, Jr., "Survey of thermal, radiation, and viscous damping of pulsating air bubbles in water," J. Acoust. Soc. Am. **31**, 1654 (1959).
[3] R. His, M. Tay, D. Bukur, and G. Tatterson, "Sound spectra of gas dispersion in an agitated tank," Chem. Eng. J. **31**, 153–161 (1985).
[4] L. S. De More, W. F. Pafford, and G. B. Tatterson, "Cavity sound resonance and mass transfer in aerated agitated tank," AIChE J. **34**, 1922–1926 (1988).
[5] J. W. R. Boyd and J. Varley, "Sound measurement as a means of gas-bubble sizing in aerated agitated tank," AIChE J. **44**, 1731–1739 (1998).
[6] A. B. Pandit, J. Varley, R. B. Thorpe, and J. F. Davidson, "Measurement of bubble size distribution: An acoustic technique," Chem. Eng. Sci. **47**, 1079–1089 (1992).
[7] R. Manasseh, R. F. LaFontaine, J. Davy, I. Shepherd, and Y-G Zhu, "Passive acoustic bubble sizing in sparged systems," Exp. Fluids (in press).
[8] R. Manasseh, A. Bui, J. Sandercock, and A. Ooi, "Sound emission processes on bubble detachment," Proceedings of the 14th Australasian Fluid Mechanics Conference (in press).
[9] T. A. Sutter, G. L. Morrison, and G. B. Tatterson, "Sound spectra in an aerated agitated tank," AIChE J. **33**, 668–671 (1987).
[10] W. R. Usry, G. L. Morrison, and G. B. Tatterson, "On the interrelationship between mass transfer and sound spectra in an aerated agitated tank," Chem. Eng. Sci. **42**, 1856–1859 (1987).
[11] T. G. Leighton, D. G. Ramble, A. D. Phelps, C. L. Morfey, and P. P. Harris, "Acoustic detection of gas bubbles in a pipe," Acta Acust. **84**, 801–814 (1998).
[12] H. Pfriem, "Zur thermischen dämpfung in kugelsymmetrisch schwingenden gasblasen," Akust. Zh. **5**, 202–207 (1940).
[13] Z. Saneyoshi, Electro-technical Journal (Japan) **5**, 49 (1941).
[14] A. I. Eller, "Damping constants of pulsating bubbles," J. Acoust. Soc. Am. **47**, 1469–1470 (1970).
[15] A. Prosperetti, "Thermal effects and damping mechanisms in the forced radial oscillations of gas bubbles in liquids," J. Acoust. Soc. Am. **61**, 17–27 (1977).
[16] R. I. Nigmatulin and N. S. Khabeev, "Heat exchange between a gas bubble and a liquid," Fluid Dyn. **9**, 759–764 (1974).
[17] R. I. Nigmatulin and N. S. Khabeev, "Dynamics of vapour-gas bubbles," Fluid Dyn. **12**, 867–871 (1977).
[18] F. B. Nagiev and N. S. Khabeev, "Heat-transfer and phase transition effects associated with oscillations of vapour-gas bubbles," Sov. Phys. Acoust. **25**, 148–152 (1979).
[19] R. I. Nigmatulin, N. S. Khabeev, and F. B. Nagiev, "Dynamics, heat and mass transfer of vapour-gas bubbles in a liquid," Int. J. Heat Mass Transf. **24**, 1033–1044 (1981).
[20] A. Prosperetti, L. A. Crum, and K. W. Commander, "Nonlinear bubble dynamics," J. Acoust. Soc. Am. **83**, 502–514 (1988).
[21] A. Prosperetti, "The thermal behaviour of oscillating gas bubbles," J. Fluid Mech. **222**, 587–616 (1991).
[22] P. M. Morse and K. U. Ingard, *Theoretical Acoustics* (Princeton University Press, Princeton, 1986), 555 pp.
[23] This mode, if it exists, is labeled $N=0$. It corresponds to a uniform pressure $p_0(\mathbf{x})=\rho c^2 U/j\omega V$. Its contribution in the limit $k_0\to 0$ (i.e., $\omega\to 0$) would be infinite. Since we are dealing with a tank containing a free surface, there is no $N=0$ mode.
[24] This approximation requires $K_N R \ll 1$, and so sets an upper limit to K_N, or equivalently an upper limit to N in the summation. However the limitation becomes important for Z, only if $k_0 R$ is not much less than unity, and therefore will not apply to this paper because the condition $k_0 R \ll 1$ was stated at the outset.
[25] T. G. Leighton, *The Acoustic Bubble* (Academic Press, New York, 1994), Sec. 3.2.1c(iii), 3.3.1(b), 3.5.2, 3.7.3.
[26] M. Rowan-Robinson, *Cosmology*, 2nd ed. (Oxford University Press, Oxford, 1981), p. 56.
[27] T. G. Leighton, A. D. Phelps, D. G. Ramble, and D. A. Sharpe, "Comparison of the abilities of eight acoustic techniques to detect and size a single bubble," Ultrasonics **34**, 661–667 (1996).
[28] J. K. Hammond, "Fundamentals of signal processing," in *Fundamentals of Noise and Vibration*, edited by F. J. Fahy and J. Walker (E&FN Spon, London, 1998), Chap. 6, pp. 311–370.
[29] T. G. Leighton, K. J. Fagan, and J. E. Field, "Acoustic and photographic studies of injected bubbles," Eur. J. Phys. **12**, 77–85 (1991).
[30] A. R. Kolaini, L. A. Crum, and R. A. Roy, "Bubble production by capillary-gravity waves," J. Acoust. Soc. Am. **95**, 1913–1921 (1994).
[31] A. R. Kolaini, "Effects of salt on bubble radiation," in *Natural Physical Processes Associated with Sea Surface Sound*, edited by T. G. Leighton (University of Southampton, Southampton, 1997), pp. 240–249.
[32] A. R. Kolaini, "Sound radiation by various types of laboratory breaking waves in fresh and salt water," J. Acoust. Soc. Am. **103**, 300–308 (1998).
[33] A. R. Kolaini and L. A. Crum, "Observations of underwater sound from laboratory breaking waves and the implications concerning ambient noise in the ocean," J. Acoust. Soc. Am. **96**, 1755–1765 (1994).
[34] J. A. Kitchener, "Foams and free liquid film," *Recent Progress in Surface Science* (Academic, New York, 1964), Vol. I, pp. 51–93.
[35] E. C. Monahan and C. R. Zeitlow, "Laboratory comparisons of fresh-water and salt-water whitecap," J. Geophys. Res. **74**, 6961–6966 (1969).
[36] J. C. Scott, "The role of salt in whitecap persistence," Deep-Sea Res. Oceanogr. Abstr. **22**, 653–657 (1975).
[37] S. A. Thorpe, "The role of bubbles produced by breaking waves in supersaturating the near-surface ocean mixing layer with oxygen," Ann. Geophys. (Gauthier-Villars, 1983–1985) **2**, 53–56 (1984).
[38] L. Memery and L. Merlivat, "Modeling of gas flux through bubbles at the air-water interface," Tellus, Ser. B **37B**, 272–285 (1985).
[39] C. Pounder, "Sodium chloride and water temperature effects on bubbles," in *Oceanic Whitecap and Their Role in Air-Sea Exchange Processes*, edited by E. C. Monahan and G. Mac Niocaill (Reidel, Dordrecht, 1986).
[40] W. M. Carey, J. W. Fitzgerald, E. C. Monohan, and Q. Wang, "Measurement of the sound produced by a tipping trough with fresh and salt water," J. Acoust. Soc. Am. **93**, 3178–3192 (1993).
[41] A. R. Kolaini (personal communication).
[42] N. Breitz and H. Medwin, "Instrumentation for *in situ* acoustical measurements of bubble spectra under breaking waves," J. Acoust. Soc. Am. **86**, 739–743 (1989).
[43] D. M. Farmer and S. Vagle, "Waveguide propagation of ambient sound in the ocean-surface bubble layer," J. Acoust. Soc. Am. **86**, 1897–1908 (1989).
[44] A. D. Phelps, D. G. Ramble, and T. G. Leighton, "The use of a combination frequency technique to measure the surf zone bubble population," J. Acoust. Soc. Am. **101**, 1981–1989 (1997).
[45] W. K. Melville, E. Terrill, and F. Veron, "Bubbles and turbulence under breaking waves," in *Natural Physical Processes Associated with Sea Surface Sound*, edited by T. G. Leighton (University of Southampton, Southampton, 1997), pp. 135–146.
[46] I. N. Didenkulov, S. I. Muyakshin, and D. A. Selivanovsky, "Bubble counting in the subsurface ocean layer," in *Acoustical Oceanography*, Proceedings of the Institute of Acoustics, Vol. 23 Part 2, 2001, edited by T. G. Leighton, G. J. Heald, H. Griffiths, and G. Griffiths (Institute of Acoustics, 2001), pp. 220–226.
[47] V. A. Akulichev, V. A. Bulanov, and S. A. Klenin, "Acoustic sensing of gas bubbles in the ocean medium," Sov. Phys. Acoust. **32**, 177–180 (1986).
[48] J. L. Leander, "A note on transient underwater bubble sound," J. Acoust. Soc. Am. **103**, 1205–1208 (1998).
[49] J. W. L. Clarke and T. G. Leighton, "A method for estimating time-dependent acoustic cross-sections of bubbles and bubble clouds prior to the steady state," J. Acoust. Soc. Am. **107**, 1922–1929 (2000).
[50] S. D. Meers, T. G. Leighton, J. W. L. Clarke, G. J. Heald, H. A. Dumbrell, and P. R. White, "The importance of bubble ring-up and pulse length in estimating the bubble distribution from propagation measurements," in Ref. 46, pp. 235–241.
[51] J. L. Spiesberger and K. Metzger, "New estimates of sound speed in water," J. Acoust. Soc. Am. **89**, 1697–1700 (1991).
[52] Equation (43) was used to correct for reverberation in the surf zone by T. G. Leighton, "Surf zone bubble spectrometry: The role of the acoustic cross section," J. Acoust. Soc. Am. **110**, 2694 (2001).
[53] N. Breitz and H. Medwin, "Instrumentation for *in situ* acoustical measure-

ments of bubble spectra under breaking waves,'' J. Acoust. Soc. Am. **86**, 739–743 (1989).
[54] M. Y. Su, D. Todoroff, and J. Cartmill, ''Laboratory comparisons of acoustical and optical sensors for microbubble measurement,'' J. Atmos. Ocean. Technol. **11**, 170–181 (1998).
[55] D. M. Farmer, S. Vagle, and A. D. Booth, ''A free-flooding acoustical resonator for measurement of bubble size distributions,'' J. Atmos. Ocean. Technol. **15**, 1132–1146 (1998).
[56] D. F. Gaitan and L. A. Crum, ''Observation of sonoluminescence from a single cavitation bubble in a water/glycerine mixture,'' in *Frontiers of Nonlinear Acoustics, 12th ISNA*, edited by M. F. Hamilton and D. T. Blackstock (Elsevier, New York, 1990), p. 459.
[57] A. I. Eller, ''Growth of bubbles by rectified diffusion,'' J. Acoust. Soc. Am. **52**, 1447–1449 (1972).
[58] L. A. Crum, ''The polytropic exponent of gas contained within air bubbles pulsating in a liquid,'' J. Acoust. Soc. Am. **73**, 116–120 (1983).
[59] L. A. Crum and A. Prosperetti, ''Nonlinear oscillations of gas bubbles in liquids: An interpretation of some experimental results,'' J. Acoust. Soc. Am. **73**, 121–127 (1983).